INTERNATIONAL JOURNAL OF CLIMATOLOGY
*Int. J. Climatol.* **33**: 793–805 (2013)
Published online 15 March 2012 in Wiley Online Library
(wileyonlinelibrary.com) DOI: 10.1002/joc.3464

RMetS
Royal Meteorological Society

# Development of a multimodel-based seasonal prediction system for extreme droughts and floods: a case study for South Korea

Soo-Jin Sohn,[a,b]* Chi-Yung Tam[c] and Joong-Bae Ahn[b]
[a] *APEC Climate Center (APCC), Busan, Republic of Korea*
[b] *Pusan National University, Busan, Republic of Korea*
[c] *Guy Carpenter Asia-Pacific Climate Impact Centre, School of Energy and Environment, City University of Hong Kong, Hong Kong, China*

**ABSTRACT:** An experimental, district-level system was developed to forecast droughts and floods over South Korea to properly represent local precipitation extremes. The system is based on the Asia-Pacific Economic Cooperation (APEC) Climate Center (APCC) multimodel ensemble (MME) seasonal prediction products. Three-month lead precipitation forecasts for 60 stations in South Korea for the season of March to May are first obtained from the coarse-scale MME prediction using statistical downscaling. Owing to the relatively small variance of the MME and regression-based downscaling outputs, the downscaled MME (DMME) products need to be subsequently inflated. The final station-scale precipitation predictions are then used to produce drought and flood forecasts on the basis of the Standardized Precipitation Index (SPI).

The performance of three different inflation schemes was also assessed. Of these three schemes, the method that simply rescales the variance of predicted rainfall to that based on climate records, irrespective of the prediction skill or the DMME variance itself at a particular station, gives the best overall improvement in the SPI predictions. However, systematic biases in the prediction system cannot be removed by variance inflation. This implies that DMME techniques must be further improved to correct the bias in extreme drought/flood predictions. Overall, it is seen that DMME, in conjunction with variance inflation, can predict hydrological extremes with reasonable skill. Our results could inform the development of a reliable early warning system for droughts and floods, which is invaluable to policy makers and stakeholders in agricultural and water management sectors, and so forth and is important for mitigation and adaptation measures. Copyright © 2012 Royal Meteorological Society

KEY WORDS SPI; MME; statistical downscaling; variance inflation; seasonal prediction; extreme droughts and floods

*Received 4 October 2011; Revised 20 January 2012; Accepted 12 February 2012*

## 1. Introduction

Extreme droughts and floods result in tremendous economical, social, and environmental losses. Overall, drought is one of the costliest types of natural disasters and affects many people every year (Wilhite, 2000). The 1994–1995 drought in South Korea, caused by a large-scale circulation system rather than local factors (Park and Schubert, 1997), affected an area of 173 269 ha (MCT, 1995). During 2011, 86 cities and approximately 300 000 people were affected by the most severe drought (KWRA, 2002) to have struck South Korea during the last 100 years ('Seoul, 10 June 2011 (Agence France-Press)', available at http://reliefweb.int/node/81 940; Min *et al*., 2003; Sohn *et al*., 2011b). The drought was induced by an anomalous high at the centre of the Eurasian continent (Lee *et al*., 2001). In July 2011, an extremely severe flood event hit South Korea, with Seoul recording the heaviest single-day rainfall since 1907 (available at www.ncdc.noaa.gov/climate-monitoring). El Niño and Southern Oscillation (ENSO) events, including its recently discovered flavour called, ENSO Modoki, also strongly influence the hydrological cycle in many Asia-Pacific locations (Ashok *et al*., 2007, 2009; Weng *et al*., 2007; Zhang *et al*., 2007; Feng *et al*., 2010; Pradhan *et al*., 2011; Sohn *et al*., 2012). Moreover, flood frequency can be quite sensitive to modest changes in climate (Knox, 1993). Developing a reliable prediction system for hydrological extremes is essential to the preparedness of stakeholders and policy makers in agricultural planning, water management, and so forth. However, there are still very few studies on seasonal predictions of extreme droughts and floods across South Korea.

In recent decades, climate and weather forecast skill has increased drastically (Goddard *et al*., 2001), and it is worthwhile to explore the potential of extreme drought and flood forecasts derived from general circulation model (GCM)-based seasonal prediction systems. GCM products have been adapted to assess potential climatic impacts on water resources at the district level (Vidal and Wade, 2009; Vosin *et al*., 2010; Kim *et al*., 2011), using

* Correspondence to: S.-J. Sohn, APEC Climate Center (APCC), 1463 U-dong, Haeundae-gu, Busan 612020, Republic of Korea.
E-mail: jeenie7@apcc21.net

bias-corrected local scaling (BLS) methods (Wood *et al.*, 2002). The procedure involves a bias correction of GCM outputs using a probability-mapping approach, before the use of simple spatial interpolation.

Recently, multimodel ensemble (MME) prediction products have also been statistically downscaled to improve the skill of local precipitation predictions at the seasonal time scale (Kang *et al.*, 2007, 2009; Chu *et al.*, 2008). There are two major advantages of using such a method to forecast local precipitation. One is that the MME approach can usually lead to more accurate forecasts owing to the better sampling of uncertainties related to model formulations (Krishnamurti *et al.*, 1999, 2000; Doblas-Reyes *et al.*, 2000; Palmer *et al.*, 2000; Shukla *et al.*, 2000). In addition, statistical post processing can lead to further reduction of model biases, and in many cases, can tap into the predictability of some local variable if the latter is related to the large-scale circulation patterns that are well resolved by GCMs (Karl *et al.*, 1990). However, there is often relatively low variance in the MME (Yoo and Kang, 2005) and regression-based downscaling prediction products (Feddersen *et al.*, 1999; von Storch, 1999; Kang *et al.*, 2004; Feddersen and Andersen, 2005). Therefore, there is a need for methods for correcting low variance such that local-level drought and flood forecasts can be realistic in both their temporal fluctuations and absolute magnitudes (Klein *et al.*, 1959; Huth, 1999; Kang *et al.*, 2004).

In this study, we seek to develop a reliable long lead, district-level MME-based prediction system for droughts and floods, using the downscaled MME (DMME) method and the inflation of the variance of the prediction products. One novelty of this approach is a more physically meaningful downscaling compared to BLS, combined with the merits of MME; another is the inflation of low variance originating from both downscaling and MME. The goal is to accurately predict springtime droughts and floods over South Korea, which comprises the southern part of the Korean Peninsula, between 33°N and 39°N and from 124°E to 130°E (Figure 1(a)). In the boreal spring, South Korea is susceptible to abnormal aridity, droughts, and dust storms. Moreover, rainfall deficiency accumulated from the previous winter can greatly impact agriculture practices such as irrigation and seeding. Thus, for mitigation and preparedness purposes, accurate forecasting of seasonal disparities (particularly extremes) in local rainfall has become an important topic for South Korea. In this article, we implement a three-step procedure to produce a long lead, district-level MME-based prediction for extreme drought and flood events: The first step is spatial downscaling of precipitation data from multiple global models to stations across South Korea. Next, variance inflation is applied, as necessary, to calibrate the amplitude of the downscaling prediction. Three different approaches to correcting the variance of the Asia-Pacific Economic Cooperation (APEC) APEC Climate Center (APCC) 3-month DMME precipitation forecasts are evaluated (an alternative method, which will not be considered in this study, is to add a stochastic noise term to the forecasts; Hewitson, 1998; Kilsby *et al.*, 1998; von Storch, 1999; Min *et al.*, 2011). The final step is to produce drought or flood forecasts on the basis of the Standardized Precipitation Index (SPI; McKee *et al.*, 1993, 1995) for each station location.

The rest of the article is organized as follows: Section 2 describes the forecast procedure and datasets used and Section 3 presents the results of downscaling, variance correction methods, and extreme drought and flood predictions across South Korea. A summary and discussion of the results are presented in Section 4.

## 2. Data and prediction procedure

### 2.1. Data

In this study, the prediction period of interest is the three months during the March–April–May (MAM) season. The retrospective forecast (hindcast) datasets span a period of 21 years, from 1983 to 2003, for the same season. Particular attention is paid to 3-month accumulated precipitation anomalies later used to calculate SPI.

These datasets are obtained from ten operational seasonal prediction models participating in the APCC MME seasonal forecast (Kang *et al.*, 2007, 2009; Lee *et al.*, 2011; Min *et al.*, 2011; Sohn *et al.*, 2011). The hindcast data generation methods examined in this study follow the guidelines of the Seasonal Model Intercomparison Project/Historical Forecast Project (Kang and Shukla, 2006) or Coupled Model Intercomparison Project (Covey *et al.*, 2003) typed experiments, with 1-month lead time, issued on 1 February. The ten prediction systems used are listed in Table I. These forecasts are used to derive a statistical relationship between the observed local-scale precipitation (i.e. predictand) and the models' behaviour on large-scale circulation (predictor) in the cross-validated mode (Michaelsen, 1987). Potential predictors include upper-air variables such as temperature at 850 hPa (T850), winds at 850/200 hPa (UV850/200), and the geopotential height at 500 hPa (Z500), as well as air temperature at 2 m (T2M), and sea-level pressure (SLP).

The baseline reference precipitation data was obtained from 60 stations in South Korea, shown in Figure 1(b); the data were used to calibrate and validate the precipitation predictions at the target locations (for more information, Table AI). In South Korea, there are two main ridges, namely, the Taebaek and Sobaek Mountains. The Taebaek Mountains are located along the eastern edge of the peninsula and run along the East Sea (average elevation approximately 1000 m). The Sobaek Mountains cut across the southern Korean Peninsula, diverge from the Taebaek Mountains, and trend southwest across the centre of the peninsula.

### 2.2. Hydrological extreme forecast system

#### *2.2.1. Statistical downscaling*

Local precipitation forecasts at 60 stations in South Korea are produced using statistical downscaling, which

 

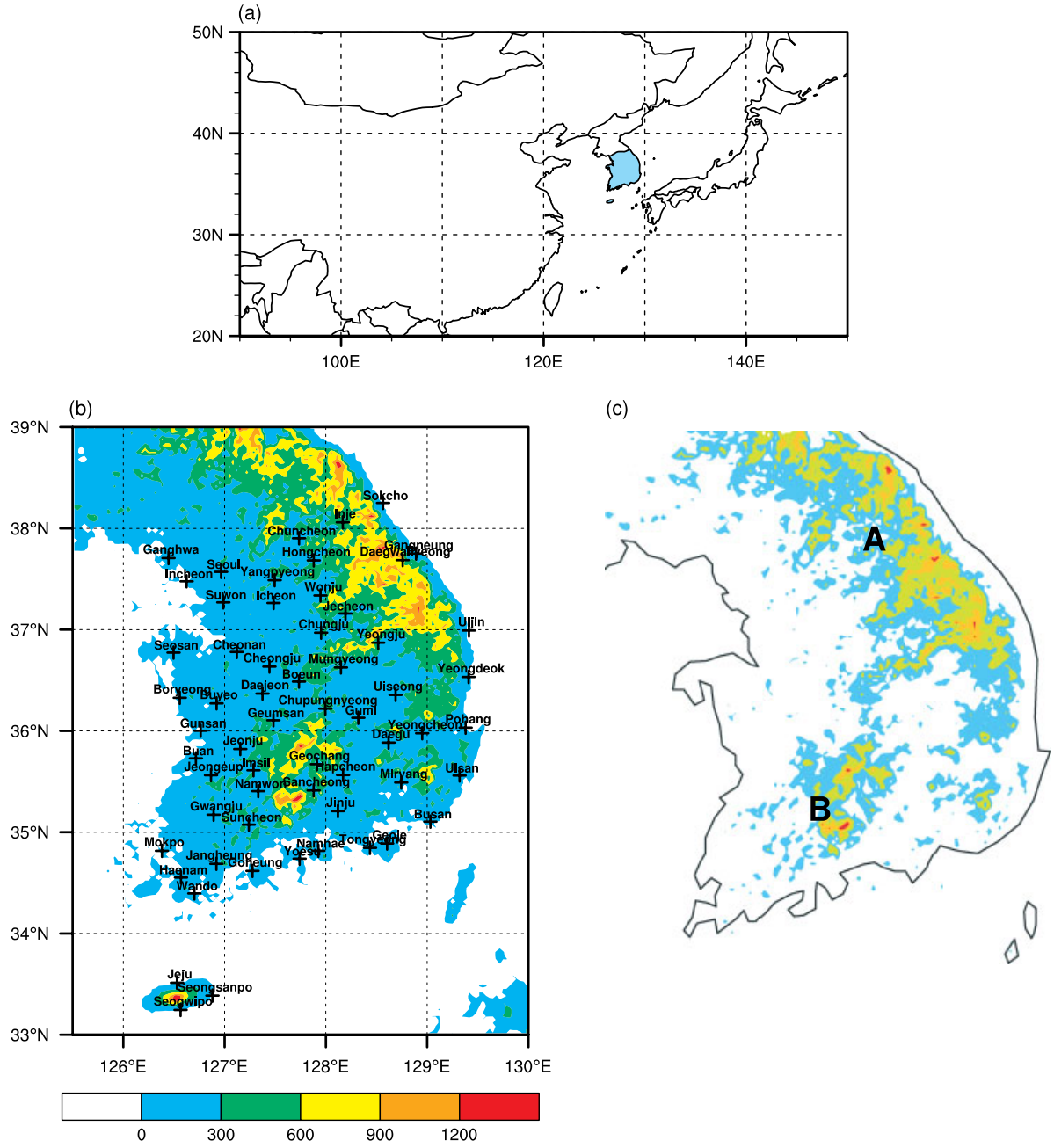


Figure 1. (a) East Asia with South Korea indicated by shading, (b) topographic map (shaded; units: m) with the locations of 60 stations (marked with crosses) considered in the study, and (c) locations of the (A) Taebaek and (B) Sobaek Mountains.

is a regression-based method with multimodel output variables as predictors (Kang *et al*., 2009). This method consists of the following steps: (1) coupled pattern selection and projection (Kang *et al*., 2007; Kug *et al*., 2007), (2) selection of optimal multipredictors, and (3) multimodel averaging. A downscaled retrospective prediction by (1) and (2) is produced separately for each model on the basis of a leave-one-out cross-validation framework. The pattern projection method selects the optimal predictor for each station by performing global scanning of different variables. The final forecast obtained from (3) is then the simple average of downscaled precipitation forecasts of the ten models using their respective optimal predictors.

### 2.2.2. *Variance inflation*

At time '$t$', the DMME prediction at a particular station '$k$', denoted by $Y_{(t,k)}$, is inflated to $Z_{(t,k)}$ according to the following formula:

$$Z_{(t,k)} = Y_{(t,k)} \times \mathrm{IF}_{(k)},$$

where $\mathrm{IF}_{(k)}$ represents the inflation factor. Three possible methods of variance correction, i.e. ways to define the inflation factor IF, were tested in predicting extreme hydrological events over South Korea. Along with the original non-inflated DMME precipitation forecast, we tested four different methods for predicting hydrological

 

Table I. Description of the general circulation models used in this study.

| Model acronym | Institution (country) | Resolution | Ensemble size | Model experiment for hindcast generation | Reference |
|---|---|---|---|---|---|
| BCC | Beijing Climate Center (BCC) | T63 L16 | 8 | CMIP | Ding *et al.* (2000) |
| CWB | Central Weather Bureau (Chinese Taipei) | T42 L18 | 10 | SMIP/HFP | Liou *et al.* (1997) |
| GCPS | Seoul National University (Korea) | T63 L21 | 12 | SMIP/HFP | Kang *et al.* (2004) |
| GDAPS | Korea Meteorological Administration (Korea) | T106 L21 | 20 | SMIP/HFP | Park *et al.* (2002) |
| MSC GM2 | Meteorological Service of Canada (Canada) | T32 L10 | 10 | SMIP/HFP | McFarlane *et al.* (1992) |
| MSC GM3 | Meteorological Service of Canada (Canada) | T63 L32 | 10 | SMIP/HFP | Scinocca *et al.* 2008 |
| MSC SEF | Meteorological Service of Canada (Canada) | T95 L27 | 10 | SMIP/HFP | Ritchie (1991) |
| NIMR | National Institute of Meteorological Research (Korea) | $5^\circ \times 4^\circ$ L17 | 10 | SMIP/HFP | Back *et al.* (2002) |
| NCEP CFS | NCEP Climate Prediction Center (USA) | T62 L64 | 15 | CMIP | Saha *et al.* (2006) |
| POAMA | Bureau of Meteorology Research Center (Australia) | T47 L17 | 10 | CMIP | Zhong *et al.* (2005) |

CMIP, Coupled Model Intercomparison Project; SMIP/HFP, Seasonal Model Intercomparison Project/Historical Forecast Project

Table II. Variance correction methods.

| Abbreviation | Formula | Reference |
|---|---|---|
| M1 | $\mathrm{IF}_{(k)} = 1/\mathrm{Corr}(\mathrm{FCST}(k), \mathrm{OBS}(k))$ | Klein *et al.* (1959)<br>Karl *et al.* (1990)<br>Huth (1999) |
| M2 | $\mathrm{IF}_{(k)} = \frac{\sigma_{\mathrm{OBS}(k)}}{\sigma_{\mathrm{FCST}(k)}}$ | Leung *et al.* (1999) |
| M3 | $\mathrm{IF}_{(k)} = \frac{\sigma_{\mathrm{OBS}(k)}}{\sigma_{\mathrm{FCST}(k)}} \times W\left(\frac{\sigma_{\mathrm{FCST}(k)}}{\max(\sigma_{\mathrm{FCST}(k)})}\right) W(x) = \{1 + \tan h[6.9(x - 0.5)]\}/2$ | Feddersen *et al.* (1999)<br>Kang *et al.* (2004) |

$Y_{(t,k)}$ and $Z_{(t,k)}$ are, respectively, the original and calibrated monthly mean anomalies, for station $k$ at time $t$, where $\mathrm{IF}_{(k)}$ represents the inflation factor

extremes. The formulas of the various inflation schemes are listed in Table II.

The first method of correcting variance, hereafter referred to as M1, is to inflate the forecast by a factor that is inversely proportional to the correlation between the original and downscaled time series (Klein *et al.*, 1959; Karl *et al.*, 1990; Huth, 1999). The second method (referred to as M2) is to multiply the adjusted values by the ratio between the standard deviation (SD) of the observations and that of the adjusted values (Leung *et al.*, 1999). The third way (referred to as M3) to introduce an inflation factor is by combining the common method of inflation with a weighting factor (Kang *et al.*, 2004), which depends on the magnitude of local variability of the adjusted field (Feddersen *et al.*, 1999). This approach leaves points of small variability, which usually have little skill, non-inflated while concentrating on locations with large variability.

### 2.2.3. *Calculation of SPI*

Hydrological extremes are indentified on the basis of SPI, which is a widely used index adopted by the World Meteorological Organization (WMO) for drought monitoring (WMO Press Release No. 872; Sohn *et al.*, 2011b). It can be used to detect drought over a variety of time scales and can distinguish regions with persistent or emerging hydrological extremes. SPI has the following properties (Vidal and Wade, 2009): SPI calculation is more flexible and efficient than calculations using other indices (Hayes *et al.*, 1999), and the required data are easily available (Paulo and Pereira, 2006) for achieving skill comparable with that achieved with other indices (Morid *et al.*, 2006). It can accommodate different time scales (McKee *et al.*, 1995) and tends to provide reasonable spatial consistency (Loukas and Vasiliades, 2004). It was also successfully tested in many regions (Ntale and Gan, 2003; Sonmez

 

*et al.*, 2005; Vicente-Serrano and Lopez-Moreno, 2005; Wu *et al.*, 2007).

The value of SPI is estimated by transforming the observed rainfall distribution for the most recent 30 years (here, 21 years), usually fitted to a gamma distribution, into a standardized normal distribution on an equal-probability basis (McKee *et al.*, 1993; Edwards, 1997). The two-parameter gamma distribution is defined by its frequency or probability density function:

$$g(x) = \frac{1}{\beta^{\alpha}\Gamma(\alpha)} x^{\alpha-1} e^{-x/\beta} \text{for } x < 0.$$

Here, $\alpha$ and $\beta$, both being non-negative, are the shape and scale parameters, respectively; $x$ is the precipitation amount; and $\Gamma(\alpha) = \int_0^{\infty} y^{\alpha-1} e^{-y} \mathrm{d}y$ is the gamma function. The obtained parameters are then used to find the cumulative probability of an observed precipitation event for the given month and time scale for the region in question. The cumulative probability is given by the following:

$$G(x) = \int_0^{\infty} g(x)\mathrm{d}x = \frac{1}{\hat{B}^{\hat{\alpha}}\Gamma(\hat{\alpha})} \int_0^{\infty} x^{\hat{\alpha}-1} e^{-x/\hat{\beta}} \mathrm{d}x.$$

Setting $t = x/\hat{\beta}$ gives the incomplete gamma function $G(x) = \frac{1}{\Gamma(\hat{\alpha})} \int_0^x t^{\hat{\alpha}-1} e^{-t} \mathrm{d}t$. Since the gamma function is undefined for $x = 0$ and a precipitation distribution may contain zeros, the cumulative probability is given by $H(x) = q + (1 - q)G(x)$, where $q$ is the probability of a zero. The cumulative probability, $H(x)$, is then transformed to the standard normal random variable $Z$ with mean of zero and variance of one, where $Z$ represents the value of SPI.

The advantage of using the SPI is that it recognizes a variety of time scales and provides information on precipitation deficit, precipitation percent of average, and probability. Since the SPI is normalized, wetter and drier climates can be represented in the same way. Depending on the purpose, the SPI can also be computed in a similar way with different inputs such as snowpack, stream flow, reservoir storage, soil moisture, and ground water.

On the basis of this index, extreme droughts and floods can be categorized accordingly (Table III). In particular, SPI values in the ranges of −1.0 to −1.49, −1.5 to −2.0, and less than -2.0 indicate moderate, severe, and extreme drought conditions, respectively. This study considers SPI computed for a 3-month period (hereafter referred to as SPI3) since this represents the typical time scale for precipitation deficits to affect usable water sources and soil moisture important for agriculture (McKee *et al.*, 1993).

#### 2.2.4. *Forecast quality measures*

The basic statistics of seasonal precipitation predictions for extreme droughts and floods were compared with those from observations. The forecast quality measures used include the temporal correlation coefficient (TCC), pattern correlation, SDs, probability distribution functions (PDFs), cumulative density functions (CDFs), and the interquartile range (IQR; Wilks, 1995). TCC is a skill score commonly used to assess seasonal predictive skill (Barnston, 1994). For the computation of PDFs and CDFs, we use the 3-month accumulated precipitation aggregated for 60 stations, based on a 21-year record to include more samples (Min *et al.*, 2011). IQR is defined as the difference between the upper and lower quartiles; it is the simplest, most common, and robust measure of the spread of data. Since the ultimate goal is to predict SPI3, we only consider 3-month accumulated precipitation during MAM as inputs for SPI calculations.

Table III. Flood/drought conditions categorized according to the Standardized Precipitation Index (SPI) value and corresponding class probabilities.

| SPI values | Category | Probability (%) | Cumulative frequency |
|---|---|---|---|
| >2.0 | Extremely wet | 2.3 | 1.000 |
| 1.5 to 1.99 | Very wet | 4.4 | 0.977 |
| 1.0 to 1.49 | Moderately wet | 9.2 | 0.933 |
| −0.99 to 0.99 | Near normal | 68.2 | 0.841 |
| −1.0 to −1.49 | Moderately dry | 9.2 | 0.159 |
| −1.5 to −1.99 | Severely dry | 4.4 | 0.067 |
| < − 2.0 | Extremely dry | 2.3 | 0.023 |

## 3. Results

### 3.1. Statistical downscaling

Figure 2 compares TCC between observations and the MME average of raw GCM prediction, and that based on DMME prediction, for 3-month accumulated rainfall at each station in MAM. MME products are spatially interpolated onto the 60 station locations for comparison (very similar to the BLS method). From Figure 2(a), it can be seen that the MME forecast error is particularly large in two main areas. One region is near the rim of the Taebaek Mountains (hence, the low skill corresponding to stations along the eastern coastline and just to the south of the mountain range), whereas the other is to the southeast of the Sobaek Mountains, at the southern tip of the Korean Peninsula (location shown in Figure 1). The low skill corresponding to these two regions can be attributed to the relatively coarse resolutions of GCMs (Table I), as the Korean Peninsula is only two grid points wide on a 2.5° × 2.5 grid. Interpolation of GCM products to station locations can also introduce large errors. The above suggests that simple spatial interpolation of MME seasonal prediction cannot always provide reliable station-based information for users.

On the other hand, statistical downscaling can correct a large proportion of the systematic error over South Korea, even for locations over which the rainfall is strongly

 

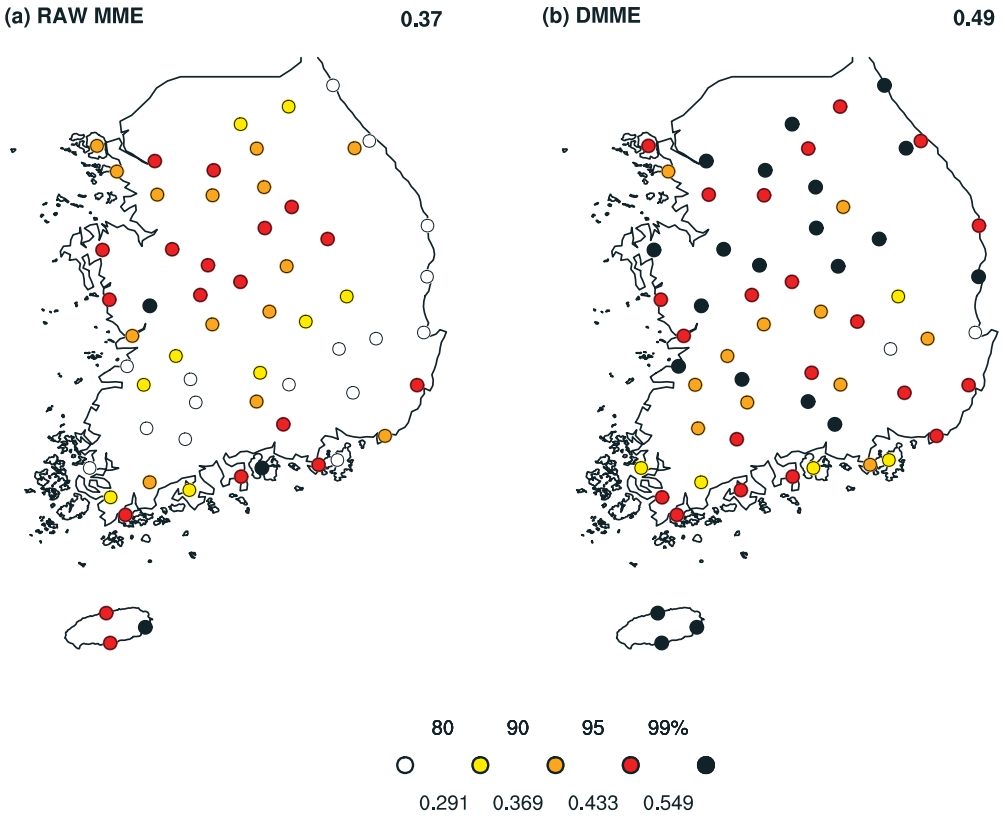


Figure 2. Temporal correlation coefficients between March–April–May accumulated precipitation anomalies from observations and those from (a) raw multimodel ensemble (MME) and (b) downscaled MME (DMME) predictions. Values with magnitudes of 0.549, 0.433, 0.352, and 0.291 represent the 99, 95, 90, and 80% significance levels, respectively. The temporal correlation, averaged over the 60 stations, is given in the upper right of each upper panel.

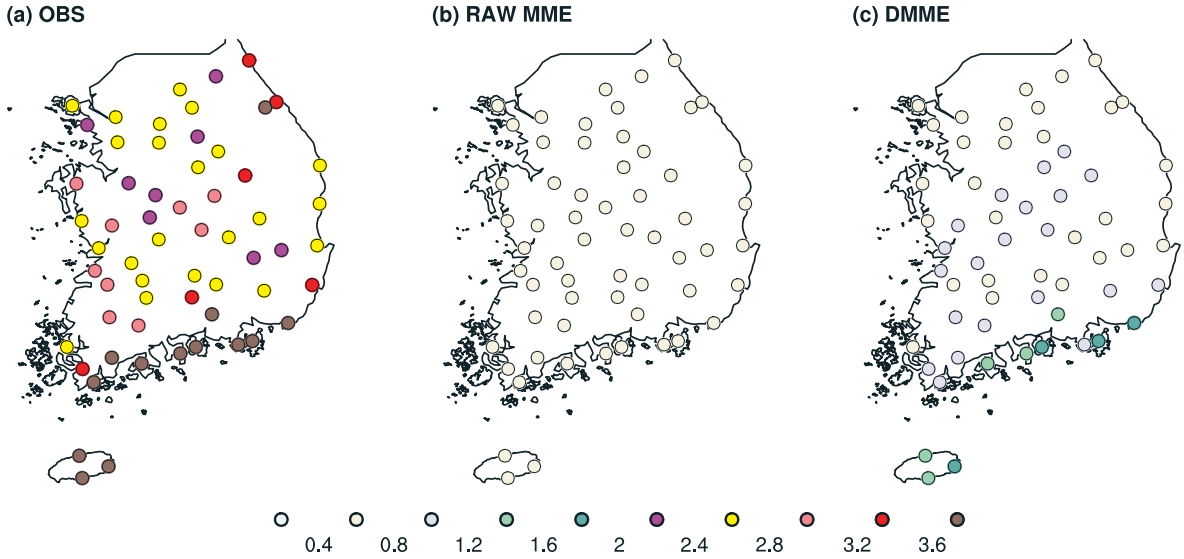


Figure 3. Interannual standard deviation for the March–April–May accumulated precipitation, based on (a) observations, (b) raw multimodel ensemble (MME), and (c) downscaled MME predictions (units: mm/d).

influenced by local topography (Kang *et al*., 2009). This is evidenced by the downscaling results in Figure 2(b). The 60-station-averaged TCC value is 0.37 based on raw MME, while it is 0.49 based on DMME. In particular, the skill corresponding to the two regions mentioned in the previous paragraph was improved by the downscaling method. Overall, DMME can significantly improve the prediction skill, as measured by the temporal correlation.

Figure 3 shows SDs of 3-month accumulated precipitation for MAM. The average accumulated spring rainfall in South Korea is approximately 80–440 mm (KMA, 2010), with some regional variations; the mean accu-

 

mulated rainfall is about 300–400 mm on the southern coast, with Jeju Island receiving more than 400 mm in spring. Figure 3(a) shows that the largest variability is found in the southern coastal locations, including Jeju Island, consistent with the mean rainfall distribution. The springtime precipitation is also influenced by the local terrain, resulting in large variability in the northeastern part of South Korea. Compared with observations, the MME average gives very low variance in precipitation (Figure 3(b)). Moreover, there is very little regional variation. For DMME, it gives larger variability in southern regions; nevertheless, the variance of the downscaling product is much less than the observed interannual variability. It is well known that the regression-based downscaling prediction tends to yield low variance (Feddersen *et al*., 1999; Kang *et al*., 2004), but this can be remedied by means of various inflation methods.

The 1983–2003 rainfall time series during spring for the whole of South Korea (i.e. averaged over 60 stations) from observations, MME, and DMME are further compared in Figure 4. It can be seen that DMME has generally better skill than MME in predicting the MAM precipitation. The observed rainfall variability is the largest, whereas both the MME and DMME give very low variance. Consistent with previous analyses, this suggests that the DMME needs to be further inflated even though it is able to capture the historical large-scale drought and flood events over South Korea.

### 3.2. Variance inflation

To compensate for the low variance of the seasonal prediction results, inflation methods are employed to adjust the amplitudes of the DMME products. Figure 5 shows the PDFs and CDFs for the 3-month accumulated precipitation aggregated for 60 stations, based on a 21-year record, for both the observations and DMME prediction results. For DMME, PDFs are computed by adding the observed climatological mean to the (inflated) downscaling station rainfall anomaly prediction. It is noteworthy that, the inflated DMMEs all give Gaussian-like PDFs that are right skewed, consistent with observations (Figure 5(a)). Although M1 is one of the most common inflation methods, its performance in this study is worse than M2, although better than the non-inflated DMME result and M3. This may be because the variance inflation implicitly assumes that all local variability is related to

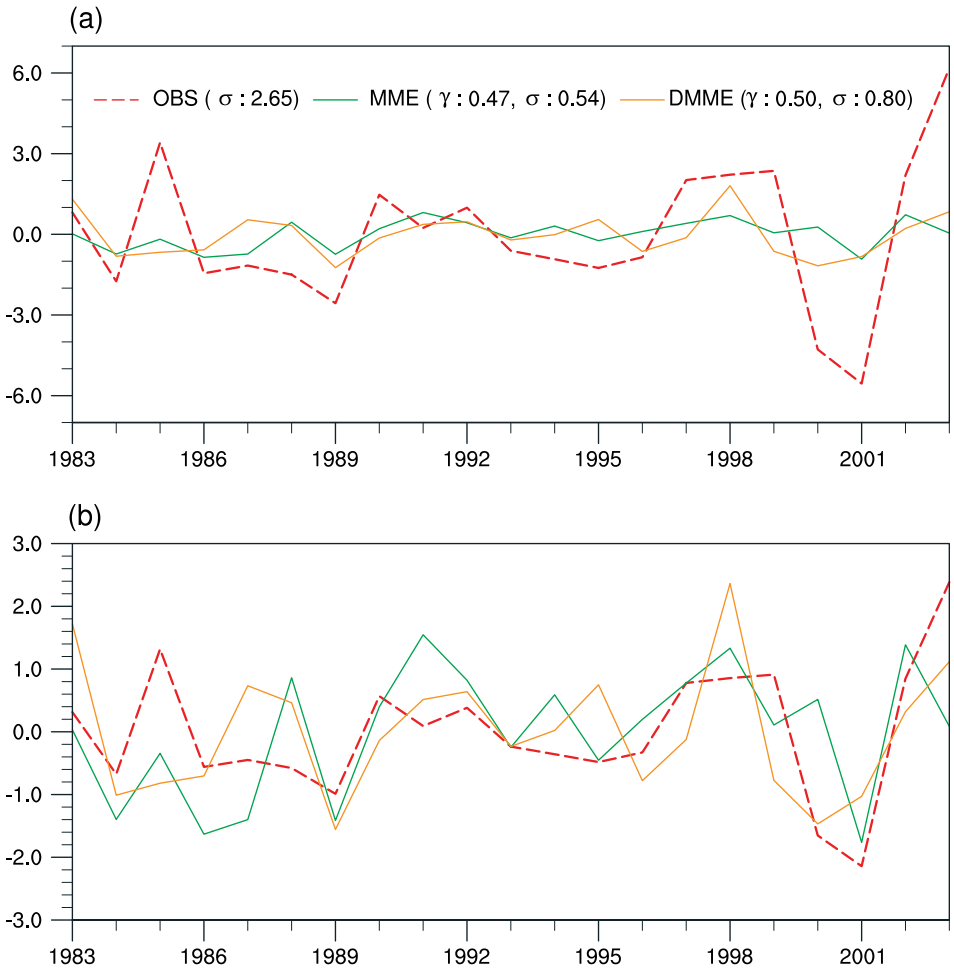


Figure 4. (a) Time series for the March–April–May accumulated precipitation anomalies, based on observations (dotted red line), raw multimodel ensemble (MME) (solid green), and downscaled MME predictions (solid orange) averaged over 60 stations; (b) same as (a) but for the standardized values. Correlation coefficients between observations and predictions ($\gamma$) and the standard deviation ($\sigma$) of each time series are given in parentheses following the legends.

 

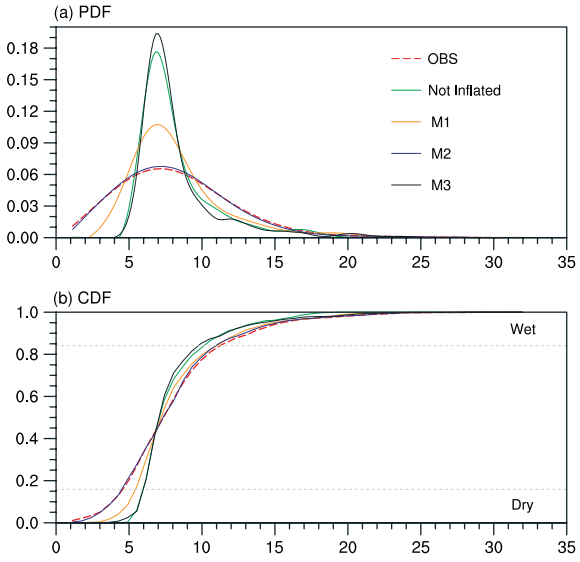


Figure 5. (a) Probability distribution functions and (b) cumulative density functions for the March–April–May accumulated precipitation from observations and various bias-corrected downscaled multimodel ensemble predictions aggregated over 60 stations.

large-scale variability, which is not the case (von Storch, 1999). Alternatively, it could be that the inflation factor is not a reciprocal of the correlation between observations and DMME prediction, especially since precipitation is not one of the potential predictors. M2 gives the best PDF and is able to reproduce extremely intensive as well as rare rainfall events. M3 gives almost the same PDF as the non-inflated method. Similar to the non-inflated prediction, most values from the M3 distribution are clustered around the climatological mean value. On the basis of the CDF plots (Figure 5(b)), it can be seen that M2 gives a distribution closest to observations. In other words, the M2-inflated DMME prediction can best characterize extreme precipitation events. In comparison, M3 and non-inflated DMME have a tendency to overestimate flood events (i.e. to give false alarms) (for reference, cumulative frequencies less than 0.159 and more than 0.841 indicate moderately dry and wet conditions, respectively; see Table III).

The spatial distributions of the DMME variance inflated by various schemes are also investigated. Figure 6 shows IQR maps for different inflation schemes.

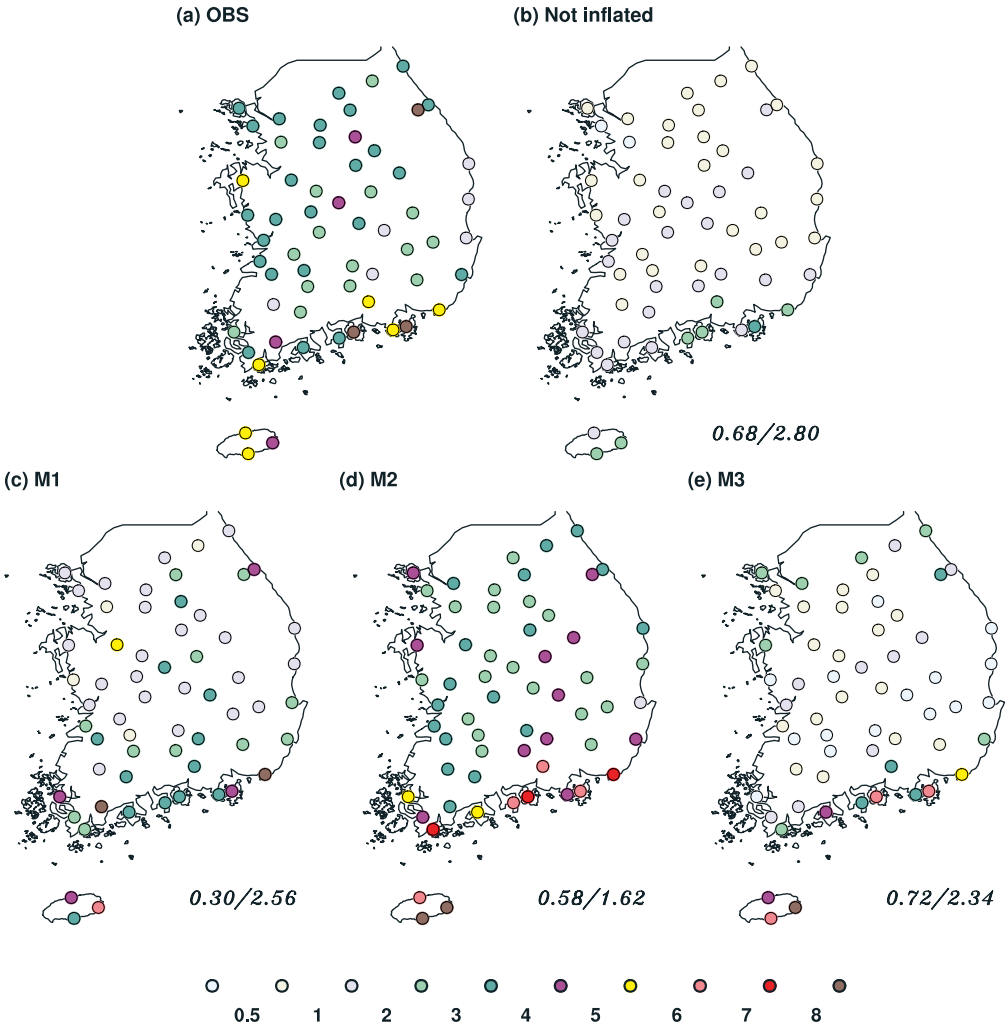


Figure 6. Interquartile ranges (IQRs) for the March–April–May accumulated precipitation for (a) observations, (b) non-inflated, (c) M1, (d) M2, and (e) M3-inflated downscaled multimodel ensemble predictions. The spatial correlation and root mean square difference between IQRs of observations and predictions are provided at the bottom right of (b) to (e).

 

It can be seen that M2, which rescales the DMME variance directly based on observations, shows a comparable spread to the observed data. The method also tends to slightly overestimate IQR in some locations. On the other hand, the non-inflated as well as the M1- and M3-inflated DMMEs tend to give smaller spreads and all give relatively large root mean square differences (about 2.3–2.8, compared to 1.6 given by M2). However, it is interesting to note that M3 shows the best spatial consistency with observations, as indicated by the high spatial correlation of 0.72. This may be because M3 leaves stations of small variability, which usually have little skill, non-inflated, while concentrating the inflation on stations with large amplitudes (Kang *et al*., 2004). It is also seen that at least M3 is good for stations with very large variability (e.g. the southern coast). Further inspection shows that the PDF of M3 in these locations is comparable with those from the other schemes, supporting the idea that M3 works better when the variance to be fitted is large (figure not shown).

### 3.3. Extreme drought and flood predictions

We now assess the impact of various calibrations of DMME precipitation forecasts on extreme drought and flood predictions. TCCs between the observed and predicted SPI3, ending in May, are given in Figure 7. SPI3 based on non-inflated DMME is moderately skilful in the northern part and the southern coastal region of South Korea (including Jeju Island). Due to its inflation method, SPI3 based on the M1 scheme actually shows a decrease in skill at some inland stations where there is a high correlation between observations and DMME (Figure 2(b)). M2 gives the best overall skill of the three schemes (based on the 60-station-averaged result), while the performance of M3 is almost the same as the non-inflated products. Overall, it appears that M2 is the best inflation method for predicting extreme drought and flood events. It is worth noting that all the schemes considered are also likely to inflate the accurate as well as inaccurate forecasts. Therefore, stations with low skill become more inaccurate when inflated by either M1, M2, or M3 (e.g. at Daegu in the southern-central part of South Korea and at Pohang near the southeastern coast).

The previous discussion focused on the average performance of different inflated DMME products over the entire period. However, it is also of interests to see how well they capture individual drought or flood episodes. Figure 8 compares the SPI maps from observations and predictions for the drought of May 2001. Most stations shows severe to extreme drought conditions, except in a few places (Figure 8(a)). A few locations also indicate moderate drought conditions. There is broad agreement between model predictions and observed conditions over the northern region of South Korea, even though the predicted signals are not as strong as the observed data. However, dry features in more southerly stations are not well captured. These systematic biases

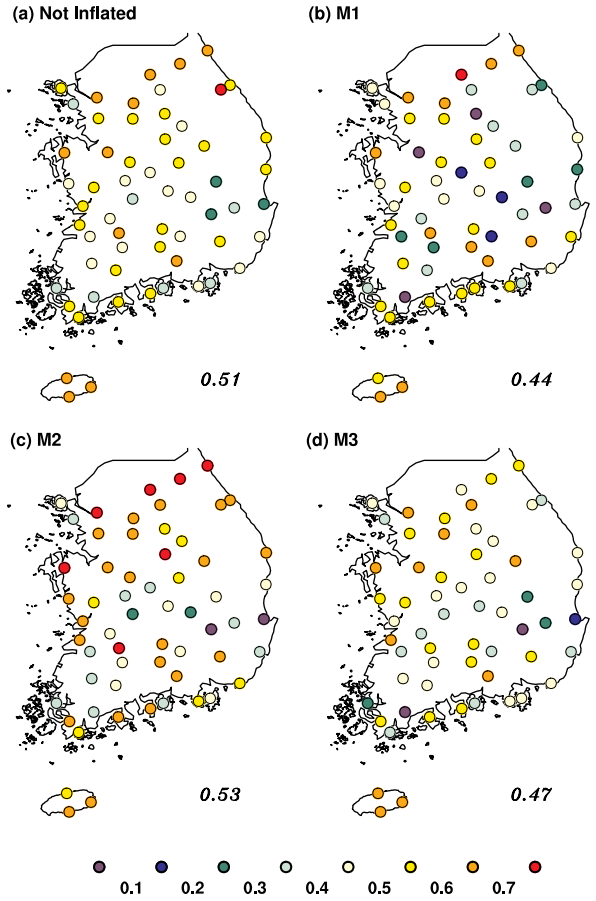


Figure 7. Temporal correlation coefficients of the standardized precipitation indices calculated for 3 months (SPI3s) ending in May during the period 1983–2003 between observations and (a) non-inflated, (b) M1, (c) M2, and (d) M3-inflated downscaled multimodel ensemble predictions. The temporal correlations averaged over 60 stations are provided at the bottom right of each panel.

cannot be solved through simple inflation. Again, the M2-inflated prediction shows the best performance of all the inflated DMME products. Finally, we also assessed the extent to which our method can predict wet episodes in South Korea. During the anomalously wet boreal spring season of 1998, the inflated DMME also give more reasonable SPI maps compared with the non-inflated prediction. In this case, the non-inflated DMME overestimated SPI values due to its smaller interannual range; the variance-corrected prediction based on M2 is seen to give more realistic SPI predictions (figure not shown).

## 4. Summary

A long lead, district-level MME-based hydrological extreme prediction system was developed to facilitate early warning of droughts and floods. Hydrological extremes are identified based on SPI maps for the preceding 3-month period using monthly precipitation at 60 south Korean stations. First, the skill of 3-month lead precipitation forecasts for each station, based on DMME, is compared with predictions interpolated from coarse-scale

 

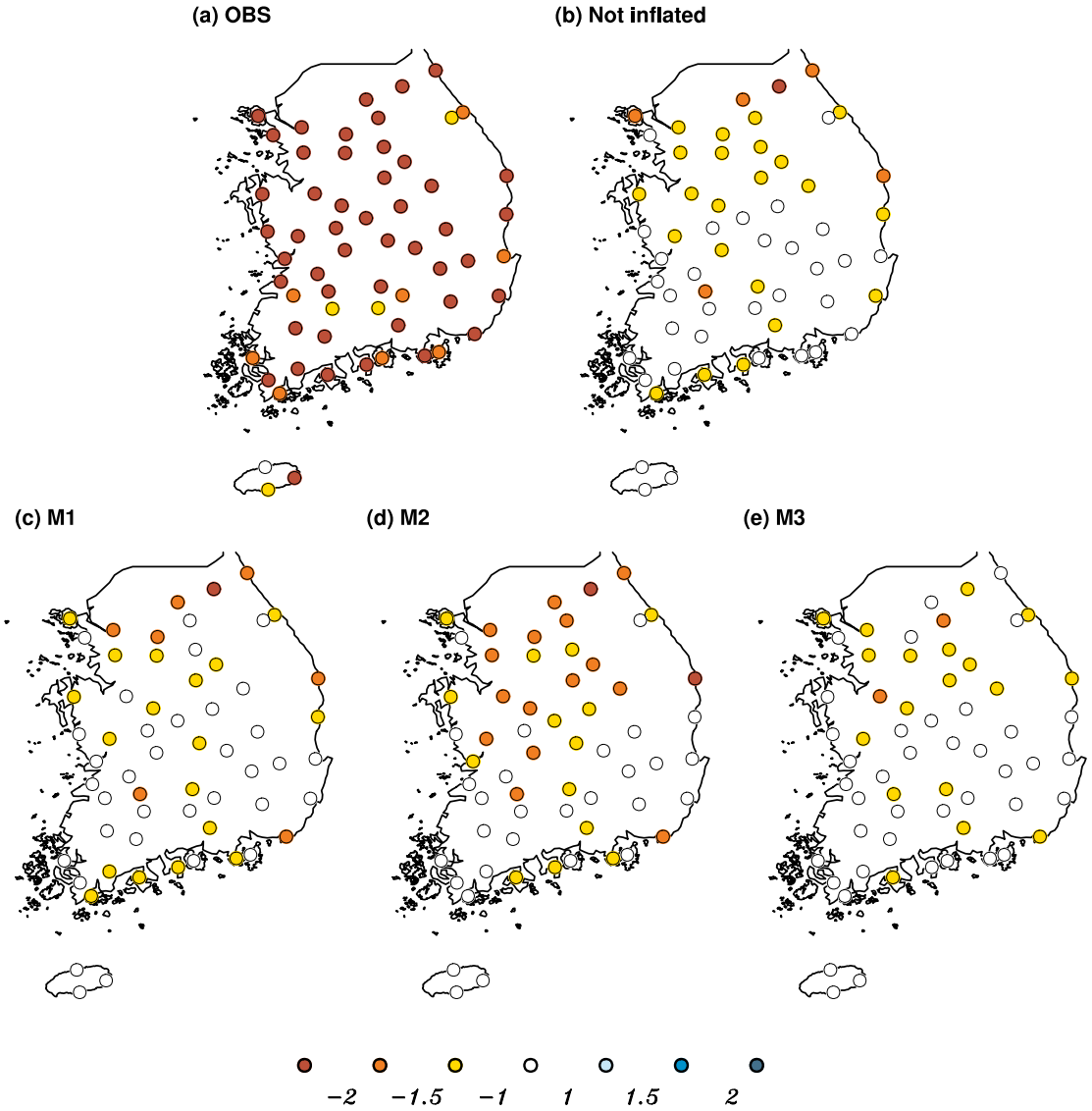


Figure 8. Standardized precipitation indices calculated for 3 months (SPI3s) ending in May 2001 from (a) observations, (b) non-inflated, (c) M1, (d) M2, and (e) M3-inflated downscaled multimodel ensemble predictions.

MME products (similar to BSL). Statistical downscaling is found to be more skilful than the raw MME, suggesting that it can be applied to more accurately assess climatic impact on water resources at the district level than the BLS method. Moreover, statistical downscaling can correct a large proportion of the systematic bias over South Korea, even for locations at which rainfall is strongly influenced by local topography.

Methods for correcting the interannual variability of DMME precipitation forecasts have also been investigated to accurately predict hydrological extreme events. In particular, the performances of three different inflation schemes were compared in improving DMME prediction. It was found that a simple rescaling of variance according to the observational record gives the best overall performance in terms of both the amplitude of precipitation variance and SPI predictions.

However, systematic biases cannot be eliminated through simple inflation itself; the application of such inflation often increases the mean square error of the estimate (Karl *et al*., 1990). The results indicate that further work is required to improve the quality of DMME forecasts of drought/flood events. For example, the improvement provided by the multimodel method is robust in regions where individual models are relatively skilful (Yoo and Kang, 2005). In general, the internal variability of the climate system, the choice of models, and the statistical downscaling models can give rise to uncertainties in model output statistics-based forecasts (Benestad, 2001; Chen *et al*., 2006). Therefore, different combinations of models and alternative downscaling methodologies should also be explored. For instance, pattern-based statistical methods, such as those using empirical orthogonal function and singular value decomposition techniques, can also be applied.

Overall, the use of DMME, in conjunction with inflation, gives very promising results in predicting extreme droughts and floods over South Korea. Our results

 

suggest that well-designed downscaling and variance inflation could be one method of utilizing meteorological forecasting to reliably predict extreme hydrological events, thereby allowing policy makers and stakeholders in the agricultural and water management sectors to develop more effective mitigation and adaption strategies. In this study, we use only the 3-month lead precipitation to represent extreme droughts and floods. Further investigations of extreme drought and flood predictions, based on longer lead times and multiple variables, will be carried out in the near future.

## Acknowledgements

We would like to thank two anonymous reviewers. Their comments resulted in significant improvements to this article. Chi-Yung Tam acknowledges the support from the City University of Hong Kong (grant no. 9360126).

## APPENDIX

Table AI. List of the synoptic stations used for the study (KMA, 2010). Height is the station elevation about mean sea level.

| Admin. Bound. | ID number | Station name | Latitude (N) | Longitude (E) | Height (m) | Starting date (dd mm yyyy) |
|---|---|---|---|---|---|---|
| Gyeonggi | 108 | Seoul | 37°34′ | 126°57′ | 85.5 | 1 October 1907 |
| | 112 | Incheon | 37°28′ | 126°37′ | 69.0 | 10 April 1904 |
| | 119 | Suwon | 37°16′ | 126°59′ | 34.5 | 1 January 1964 |
| | 201 | Ganghwa | 37°42′ | 126°26′ | 46.2 | 1 January 1971 |
| | 202 | Yangpyeong | 37°29′ | 127°29′ | 47.4 | 1 February 1971 |
| | 203 | Icheon | 37°15′ | 127°29′ | 90.0 | 1 January 1971 |
| Gangwon | 090 | Sokcho | 38°15′ | 128°33′ | 22.9 | 1 January 1968 |
| | 100 | Daegwallyeong | 37°40′ | 128°43′ | 772.4 | 11 July 1971 |
| | 101 | Chuncheon | 37°54′ | 127°44′ | 76.8 | 1 January 1966 |
| | 105 | Gangneung | 37°45′ | 128°53′ | 26.1 | 1 January 1911 |
| | 114 | Wonju | 37°20′ | 127°56′ | 150.7 | 1 September 1971 |
| | 211 | Inje | 38°03′ | 128°10′ | 198.7 | 1 September 1971 |
| | 212 | Hongcheon | 37°41′ | 127°52′ | 146.2 | 1 July 1971 |
| Chungcheongbuk | 127 | Chungju | 36°58′ | 127°57′ | 113.7 | 1 January 1971 |
| | 131 | Cheongju | 36°38′ | 127°26′ | 56.4 | 1 January 1967 |
| | 135 | Chupungnyeong | 36°13′ | 127°59′ | 240.9 | 1 September 1935 |
| | 221 | Jecheon | 37°09′ | 128°11′ | 263.1 | 1 January 1971 |
| | 226 | Boeun | 36°29′ | 127°44′ | 173.0 | 1 January 1971 |
| Chungcheongnam | 129 | Seosan | 36°46′ | 126°29′ | 25.2 | 1 January 1968 |
| | 133 | Daejeon | 36°22′ | 127°22′ | 62.6 | 1 January 1969 |
| | 232 | Cheonan | 36°46′ | 127°07′ | 21.3 | 1 January 1971 |
| | 235 | Boryeong | 36°19′ | 126°33′ | 17.9 | 1 January 1972 |
| | 236 | Buyeo | 36°16′ | 126°55′ | 11.0 | 1 January 1971 |
| | 238 | Geumsan | 36°06′ | 127°28′ | 170.6 | 1 January 1972 |
| Gyeongsangbuk | 130 | Uljin | 36°59′ | 129°24′ | 47.0 | 1 January 1971 |
| | 138 | Pohang | 36°01′ | 129°22′ | 1.3 | 1 January 1943 |
| | 143 | Daegu | 35°53′ | 128°37′ | 57.3 | 7 October 1907 |
| | 272 | Yeongju | 36°52′ | 128°31′ | 210.5 | 1 January 1971 |
| | 273 | Mungyeong | 36°37′ | 128°08′ | 170.8 | 1 January 1971 |
| | 277 | Yeongdeok | 36°31′ | 129°24′ | 41.2 | 1 December 1971 |
| | 278 | Uiseong | 36°21′ | 128°41′ | 82.6 | 1 January 1971 |
| | 279 | Gumi | 36°07′ | 128°19′ | 47.4 | 1 January 1971 |
| | 281 | Yeongcheon | 35°58′ | 128°57′ | 93.3 | 1 January 1971 |
| Gyeongsangnam | 152 | Ulsan | 35°33′ | 129°19′ | 34.6 | 1 July 1931 |
| | 159 | Busan | 35°06′ | 129°01′ | 69.2 | 9 April 1904 |
| | 162 | Tongyeong | 34°50′ | 128°26′ | 30.8 | 1 January 1967 |
| | 192 | Jinju | 35°09′ | 128°02′ | 27.1 | 1 March 1969 |
| | 284 | Geochang | 35°40′ | 127°54′ | 221.4 | 1 January 1971 |
| | 285 | Hapcheon | 35°33′ | 128°10′ | 33.0 | 1 January 1971 |
| | 288 | Miryang | 35°29′ | 128°44′ | 10.7 | 1 January 1971 |
| | 289 | Sancheong | 35°24′ | 127°52′ | 138.7 | 1 January 1971 |
| | 294 | Geoje | 34°53′ | 128°36′ | 44.5 | 1 April 1971 |
| | 295 | Namhae | 34°48′ | 127°55′ | 43.2 | 1 January 1971 |
| Jeonllabuk | 140 | Gunsan | 36°00′ | 126°45′ | 26.9 | 1 January 1968 |
| | 146 | Jeonju | 35°49′ | 127°09′ | 61.0 | 15 May 1919 |
| | 243 | Buan | 35°43′ | 126°42′ | 3.6 | 11 May 1969 |

 

(*Continued*)

| Admin. Bound. | ID number | Station name | Latitude (N) | Longitude (E) | Height (m) | Starting date (dd mm yyyy) |
|---|---|---|---|---|---|---|
| | 244 | Imsil | 35°36′ | 127°17′ | 248.0 | 11 May 1969 |
| | 245 | Jeongeup | 35°33′ | 126°51′ | 39.5 | 11 May 1969 |
| | 247 | Namwon | 35°24′ | 127°19′ | 93.5 | 1 January 1971 |
| Jeonllanam | 156 | Gwangju | 35°10′ | 126°53′ | 74.5 | 1 October 1938 |
| | 165 | Mokpo | 34°49′ | 126°22′ | 37.4 | 1 April 1904 |
| | 168 | Yoesu | 34°44′ | 127°44′ | 73.3 | 1 April 1942 |
| | 170 | Wando | 34°23′ | 126°42′ | 27.7 | 12 January 1983 |
| | 256 | Suncheon | 35°04′ | 127°14′ | 74.4 | 1 January 1972 |
| | 260 | Jangheung | 34°41′ | 126°55′ | 44.5 | 1 January 1971 |
| | 261 | Haenam | 34°33′ | 126°34′ | 4.6 | 1 February 1971 |
| | 262 | Goheung | 34°37′ | 127°16′ | 53.3 | 1 January 1971 |
| Jeju | 184 | Jeju | 33°30′ | 126°31′ | 19.9 | 1 May 1923 |
| | 189 | Seogwipo | 33°14′ | 126°33′ | 50.2 | 1 January 1961 |
| | 265 | Seongsanpo | 33°27′ | 126°5′ | 10.0 | 1 January 1971 |

## References


Ashok K, Behera SJ, Rao SA, Weng H, Yamagata T. 2007. El Niño Modoki and its possible teleconnection. *Journal of Geophysical Research* **112**: C11007. DOI: 10.1029/2006JC003798.

Ashok K, Tam CY, Lee WJ. 2009. ENSO Modoki impact on the Southern Hemisphere storm track activity during extended austral winter. *Geophysical Research Letters* **36**: L12705. DOI: 10.1029/2009GL038847.

Back SK, Ryu JH, Ryoo SB. 2002. Analysis of the CO2 doubling experiment using METRI AGCM. Part 1: the characteristics of regional and seasonal climate response. *Journal of Korean Meteorological Society* **38**: 465–477.

Barnston AG. 1994. Linear statistical short-term climate predictive skill in the Northern Hemisphere. *Journal of Climate* **7**: 1513–1564.

Benestad RE. 2001. A comparison between 2 empirical downscaling strategies. *International Journal of Climatology* **21**: 1645–1668.

Chen D, Achberger C, Raisanen J, Hellstorm C. 2006. Using statistical downscaling to quantify the GCM-related uncertainty in regional climate change scenarios: a case study of Swedish precipitation. *Advances in Atmospheric Sciences* **23**: 54–60.

Chu JL, Kang H, Tam CY, Park CK, Chen CT. 2008. Seasonal forecast for local precipitation over northern Taiwan using statistical downscaling. *Journal of Geophysical Research* **113**: D12118. DOI: 10.1029/2007JD009424.

Covey C, AchutaRao KM, Cubasch U, Jones P, Lambert SJ, Mann ME, Phillips TJ, Taylor KE. 2003. An overview of results from the coupled model intercomparison project (CMIP). *Global and Planetary Change* **37**: 103–133.

Ding Y, Ni Y, Zhang X, Li W, Dong M, Zhao ZC, Li Z, Shen W. 2000. *Introduction to the Short-Term Climate Prediction Model System.* China Meteorological Press: Beijing, China, 500 pp. (in Chinese).

Doblas-Reyes FJ, Deque M, Piedelievre JP. 2000. Multi-model spread and probabilistic seasonal forecasts in PROVOST. *Quarterly Journal of Royal Meteorological Society* **126**: 2069–2088.

Edwards DC. 1997. *Characteristics of 20th Century Drought in the United States at Multiple Time Scales*, MS thesis, Department of Atmospheric Science, Colorado State University, Fort Collins, 155 pp.

Feddersen H, Andersen U. 2005. A method for statistical downscaling of seasonal ensemble predictions. *Tellus* **57A**: 398–408.

Feddersen H, Navarra A, Wrad MN. 1999. Reduction of model systematic error by statistical correction for dynamical seasonal prediction. *Journal of Climate* **12**: 1974–1989.

Feng J, Chen W, Tam CY, Zhou W. 2011. Different impacts of El Niño and El Niño Modoki on China rainfall in the decaying phases. *International Journal of Climatology* **31**: 2091–2101. DOI: 10.1002/joc.2217.

Goddard L, Mason SJ, Zebiak SE, Ropelewski CF, Basher R, Cane MA. 2001. Current approaches to seasonal-to interannual climate prediction. *International Journal of Climatology* **21**: 1111–1152.

Hayes MJ, Svoboda MD, Wilhite DA, Vanyarkho OV. 1999. Monitoring the 1996 drought using the standardized precipitation index. *Bulletin of the American Meteorological Society* **80**(3): 429–438. DOI: 10.1175/s00382-006-0187-8.

Hewitson BC. 1998. Regional climate downscaling from GCMs. Report K751, Water Research Commission, Pretoria, South Africa.

Huth R. 1999. Statistical downscaling in central Europe: evaluation of methods and potential predictors. *Climate Research* **13**: 91–101.

Kang IS, Lee JY, Pack CK. 2004. Potential predictability of summer mean precipitation in a dynamical seasonal prediction system with systematic error correction. *Journal of Climate* **17**: 834–844.

Kang H, An K, Park CK, Solis AL, Stitthichivapak K. 2007. Multimodel output statistical downscaling prediction of precipitation in the Philippines and Thailand. *Geophysical Research Letters* **34**: L15710. DOI:10.1029/2007GL030730.

Kang H, Park CK, Saji NH, Ashok K. 2009. Statistical downscaling of precipitation in Korea using multimodel output as predictors. *Monthly Weather Review* **137**: 1928–1938. DOI: 10.1175/2008MWR2706.1.

Kang IS, Shukla J. 2006. Dynamic seasonal prediction and predictability of the monsoon. In *The Asian Monsoon*, Wang B (ed). Praxis Publishing Ltd: Chichester, UK, 787.

Karl TR, Wang WC, Schlesinger ME, Knight RW, Portman D. 1990. A method of relating general circulation model simulated climate to the observed local climate. Part I: seasonal statistics. *Journal of Climate* **3**: 1053–1079.

Kilsby CG, Cowpertwait PSP, O'Connell PE, Jones PD. 1998. Predicting rainfall statistics in England and Wales using atmospheric circulation variables. *International Journal of Climatology* **18**: 523–539.

Kim BS, Kim BK, Kwon HH. 2011. Assessment of the impact of climate change on the flow regime of the Han River basin using indicator of hydrological alteration. *Hydrological Processes* **25**(5): 691–704. DOI: 10.1002/hyp.7856.

Klein WH, Lewis BM, Enger I. 1959. Objective prediction of five-day mean temperatures during winter. *Journal of Meteorology* **16**: 672–682.

KMA. 2010. Annual climatological report. Korea meteorological administration, Seoul, Korea, 11-1360000-000016-10.

Knox JC. 1993. Large increases in flood magnitude in response to modest changes in climate. *Nature* **361**: 430–432.

Krishnamurti TN, Kishtawal CM, LaRow TE, Bachiochi DR, Zhang Z, Williford CE, Gadgil S, Surendran S. 1999. Improved weather and seasonal climate forecasts from multimodel superensemble. *Science* **285**: 1548–1550. DOI: 101126/science.285.5433.1548.

Krishnamurti TN, Kishtawal CM, Shin DW, Williford CE. 2000. Multi-model superensemble forecasts for weather and seasonal climate. *Journal of Climate* **13**: 4196–4216.

Kug JS, Lee JY, Kang IS. 2007. Global sea surface temperature prediction using a multimodel ensemble. *Monthly Weather Review* **135**: 3239–3247.

KWRA (Korean Water Resources Association). 2002. Drought record and investigation report. MCT 11-1500000-000265-14-20020630 (in Korean).


 

Lee JH, Byun YH, Park CK. 2001. The characteristics of drought in the Korean Peninsula in the spring of 2001. *Atmosphere* **11**: 342–345 (in Korean).

Lee DY, Ashok K, Ahn JB. 2011. Toward enhancement of prediction skills of multimodel ensemble seasonal prediction: a climate filter concept. *Journal of Geophysical Research* **116**: D06116. DOI: 10.1029/2010JD14610.

Leung LR, Hamlet AF, Lettenmaier DP, Kumar A. 1999. Simulations of the ENSO hydroclimate signals in the Pacific Northwest Columbia River Basin. *Bulletin of the American Meteorological Society* **80**: 2313–2329.

Liou CS, Chen JH, Terng CT, Wang FJ, Fong CT, Rosmond TE, Kuo HC, Shiao CH, Cheng MD. 1997. The second generation global forecast system at the central weather bureau in Taiwan. *Weather and Forecasting* **3**: 653–663.

Loukas A, Vasiliades L. 2004. Probabilistic analysis of drought spatiotemporal characteristics in Thessaly region, Greece. *Natural Hazards and Earth System Science* **4**: 719–731.

McFarlane NA, Boer GJ, Blanchet JP, Lazare M. 1992. The Canadian climate centre second generation general circulation model and its equilibrium climate. *Journal of Climate* **5**: 1013–1044.

McKee TB, Doesken NJ, Kleist J. 1993. The relationship of drought frequency and duration to time scales. In *Preprints of the 8th Conference on Applied Climatology.* Anaheim, 179–184.

McKee TB, Doesken NJ, Kleist J. 1995. Drought monitoring with multiple time scales. In *Preprints of the 9th Conference on Applied Climatology*. Anaheim, 233–236.

MCT (Ministry of Construction and Transportation). 1995. Drought record and investigation report. MCT 11-1500000-000264-14-19951200 (in Korean).

Michaelsen J. 1987. Cross-validation in statistical climate forecast models. *Journal of Climate and Applied Meteorology* **26**: 1589–1600.

Min SK, Kwon WT, Pak EH, Choi YG. 2003. Spatial and temporal comparisons of droughts over Korea with East Asia. *International Journal of Climatology* **23**: 223–233. DOI: 10.1002/joc.872.

Min YM, Kryjov VN, Oh JH. 2011. Probabilistic interpretation of regression-based downscaled seasonal ensemble predictions with the estimation of uncertainty. *Journal of Geophysical Research* **116**: D08101. DOI:101029/2010JD015284.

Morid S, Smakhtin V, Moghaddasi M. 2006. Comparison of seven meteorological indices for rought monitoring in Iran. *International Journal of Climatology* **26**: 971–985. DOI: 10.1002/joc.1264.

Ntale HK, Gan TY. 2003. Drought indices and their application to East Africa. *International Journal of Climatology* **23**: 1335–1357. DOI: 10.1002/joc.931.

Palmer TN, Brankovic C, Richardson DS. 2000. A probability and decision-model analysis of PROBOST seasonal multi-model ensemble integrations. *Quarterly Journal of Royal Meteorological Society* **126**: 2013–2034.

Park H, Park BK, Rah DK, Cho JY. 2002. *An improvement of global model in 2001.* KMA/NWPD Technical Report 2002-1 (In Korean).

Park CK, Schubert SD. 1997. On the nature of the 1994 East Asian summer drought. *Journal of Climate* **10**: 1056–1070.

Paulo AA, Pereira LS. 2006. Drought concepts and characterization: comparing drought indices applied at local and regional scales. *Water International* **31**: 37–49.

Pradhan PK, Preethi B, Ashok K, Krishnan R, Sahai AK. 2011. Modoki, Indian Ocean Dipole, and western North Pacific typhoons: possible implications for extreme events. *Journal of Geophysical Research* **116**: D18108. DOI: 10.1029/2011JD015666.

Ritchie H. 1991. Application of the semi-Lagrangian method to a multilevel spectral primitive-equations model. *Quarterly Journal of the Royal Meteorological Society* **117**: 91–106.

Saha S, Nadiga S, Thiaw C, Wang J, Wang W, Zhang Q, Van den Dool HM, Pan HL, Moorthi S, Behringer D, Stokes D, Peña M, Lord S, White G, Ebisuzaki W, Peng P, Xie P. 2006. The NCEP climate forecast system. *Journal of Climate* **19**: 3483–3517.

Scinocca JF, McFarlane NA, Lazare M, Li J, Plummer D. 2008. The CCCma third generation AGCM and its extension into the middle atmosphere. *Atmospheric Chemistry and Physics* **8**: 7055–7074.

Shukla J, Anderson J, Baumhefner D, Brankovic C, Chang Y, Kalnay E, Marx L, Palmer T, Paolino D, Ploshay J, Schubert S, Straus D, Suarez M, Tribbia J. 2000. Dynamical seasonal prediction. *Bulletin of American Meteorological Society* **81**: 2493–2606. DOI: 10.1175/1520-0477(2000)081<2593:DSP>2.3.CO;2.

Sohn SJ, Tam CY, Park CK. 2011a. Leading modes of East Asian winter climate variability and their predictability: an assessment of the APCC multi-model ensemble. *Journal of the Meteorological Society of Japan* **89**(5): 455–474. DOI: 10.2151/jmsj.2011-504.

Sohn SJ, Tam CY, Ashok K, Ahn JB. 2011b. Quantifying the reliability of precipitation datasets for monitoring large-scale East Asian precipitation variations. *International Journal of Climatology*. DOI: 10.1002/joc.2380 (in press).

Sohn SJ, Min YM, Lee JY, Tam CY, Kang IS, Wang B, Ahn JB, Yamagata T. 2012. Assessment of the long-lead probabilistic prediction for the Asian summer monsoon precipitation (1983–2011) based on the APCC multimodel system and a statistical model. *Journal of Geophysical Research* **117**: D04102. DOI: 10.1029/2011JD016308.

Sonmez F, Komuscu AU, Erkan A, Turgu E. 2005. An analysis of spatial and temporal dimension of drought vulnerability in Turkey using the Standardized Precipitation Index. *Natural Hazards* **35**: 243–264. DOI: 10.1007/s11069-004-5704-7.

Vicente-Serrano SM, Lopez-Moreno JI. 2005. Hydrological response to different time scales of climatological drought: an evaluation of the Standardized Precipitation Index in a mountainous Mediterranean basin. *Hydrology and Earth System Sciences* **9**: 523–533.

Vidal JP, Wade S. 2009. A multimodel assessment of future climatological droughts in the United Kingdom. *International Journal of Climatology* **29**: 2056–2071. DOI: 10.1002/joc.1843.

von Storch H. 1999. On the use of "inflation" in statistical downscaling. *Journal of Climate* **2**: 3505–3506.

Vosin N, Schaake JC, Lettenmaier DP. 2010. Calibration and downscaling methods for quantitative ensemble precipitation forecasts. *Weather and Forecasting* **25**: 1603–1627. DOI: 10.1175/2010WAF2222367.1.

Weng H, Ashok K, Behera SK, Rao SA, Yamagata T. 2007. Impacts of recent El Niño Modoki on dry/wet conditions in the Pacific rim during boreal summer. *Climate Dynamics* **29**: 113–129.

Wilhite DA. 2000. Drought as a natural hazard: Concepts and definitions. In *Drought: A Global Assessment*, Wilhite DA (ed). Routledge Publishers: London, 16.

Wilks DS. 1995. *Statistical Methods in the Atmospheric Sciences.* Academic Press: Oxford, UK, 464.

Wood AW, Maurer EP, Kumar A, Lettenmaier DP. 2002. Long-range experimental hydrologic forecasting for the eastern United States. *Journal of Geophysical Research* **107**: D20. DOI: 10.1029/2001JD000659.

Wu H, Svoboda MD, Hayes MJ, Wilhite DA, Wen F. 2007. Appropriate application of the standardized precipitation index in arid location and dry seasons. *International Journal of Climatology* **27**: 65–79. DOI: 10.1002/joc.1371.

Yoo JH, Kang IS. 2005. Theoretical examination of a multi-model composite for seasonal prediction. *Geophysical Research Letters* **32**: L18707. DOI: 10.1029/2005GL023513.

Zhang Q, Xu CY, Jiang T, Wu YJ. 2007. Possible influence of ENSO on annual maximum stream flow of the Yangtze River, China. *Journal of Hydrology* **333**: 265–274.

Zhong A, Hendon HH, Alves O. 2005. Indian Ocean variability and its association with ENSO in a global coupled model. *Journal of Climate* **18**: 3634–3649.

 